Unraveling Brittle-Fracture Statistics from Intermittent Patterns Formed During Femtosecond Laser Exposure

Christos-Edward Athanasiou,[1] Max-Olivier Hongler,[2] and Yves Bellouard[1]

[1]*Galatea Lab, STI/IMT, Ecole Fédérale Polytechnique de Lausanne (EPFL), Rue de la Maladière 71b, Neuchâtel CH-2002, Switzerland*

[2]*STI/IMT, Ecole Polytechnique Fédérale de Lausanne (EPFL), Lausanne 1015, Switzerland*

(Received 4 April 2017; revised manuscript received 30 August 2017; published 7 November 2017)

Femtosecond-laser-written patterns at the surface of brittle materials may show at random times spontaneous alternations from regular to disordered structures and vice versa. Here, we show that these random transitions carry relevant statistical information, such as the Weibull parameters characterizing the fracture of brittle materials. The regular-erratic cycles of random lengths of the observed patterns suggests a phenomenological analogy with the idle and busy periods arising in queuing systems. This analogy enables us to establish experimentally that the random durations of the successive cycles are statistically independent. Based on these observations, we propose an experimental method bypassing the need for many specimens to build up statistically relevant ensembles of fracture tests. Our method is potentially generic, as it may apply to a broad number of brittle materials.

DOI: 10.1103/PhysRevApplied.8.054013

I. INTRODUCTION

Under given femtosecond laser exposure conditions [1,2], periodic patterns with subwavelength periodicity form in the bulk of various materials. Recently [3], we reported the occurrence of intermittent transitions between periodic patterns and erratic ones appearing in lines written at the surface of the material. To produce these patterns (shown in Fig. 1), we expose a specimen translated at a constant velocity under the focus of a femtosecond laser beam carrying 270-fs pulses at a rate of 800 kHz (see Appendix A for details on the experimental setup). These line patterns are written so that the laser-affected zones intersect the surface. The transitions between organized parallel nanoplanes and randomly oriented cracks forming erratic patterns ("chaoticlike") occur abruptly and, most interesting, alternate, displaying a regenerative mechanism able to flip back from erratic patterns into highly regular ones [Fig. 1(a)]. By regenerative, we mean the restoration of the regular periodic formation of nanoplanes ("nanogratings") following an erratic sequence of disorganized fractured nanostructures.

II. PHENOMENOLOGICAL MODELING

In this paper, we explore how this spontaneously generated phenomenon can be actually used to extract information about the fracture mechanics of the surface.

Here, we formulate the hypothesis that these events find their origin in the statistical nature of the fracture. Indeed, for brittle materials, one cannot define a precise elastic limit above which they rupture. Rather, their fracture behavior is usually described by a law that defines the probability of failure at a given stress level, well captured by a Weibull distribution [4] as follows:

$$P(m, \sigma_N; \sigma) = 1 - \exp\left[-\gamma\left(\frac{\sigma}{\sigma_N}\right)^m\right]. \tag{1}$$

This probability distribution is defined by three parameters: the nominal stress σ_N, the exponential factor m, and γ–a geometrical parameter fixed by the experimental conditions (in our case, the final and initial experimental volumes tested). The two main parameters, σ_N and m, are

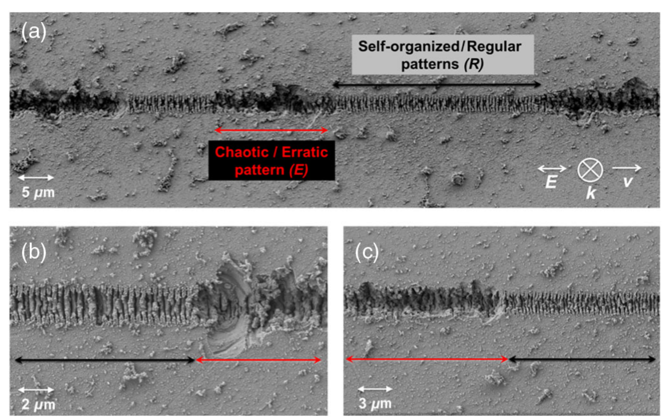

FIG. 1. (a) SEM image of the laser-processed line indicating the scanning direction (v), the laser-light polarization (E), the laser propagation direction vector (k), and the pattern that is written on the surface of a fused silica substrate. (b) and (c) show a magnified view of some line pattern transitions between regular and chaotic structures and vice versa. The black double arrows indicate regular patterns, while the red ones emphasize chaotic regimes. The pulse energy is 196 ± 1 nJ. There are about 40 pulses overlapping each unit volume producing a net fluence of 3 J/mm^2. In all these experiments, the focusing objective numerical aperture is 0.4.

determined by fitting an experimental curve derived from Eq. (1).

In previous work, we have shown that self-organized patterns are associated with a significant amount of stress introduced in the material during laser exposure [5]. Keeping in mind this observation, we formulate the general hypothesis that each single nanoplane is equivalent to loading the material to a certain stress level and, in other words, form a single "nanofracture" test experiment. Furthermore, we postulate that this phenomenon is generic and applies to a broad number of brittle materials.

The general hypothesis is based on two assumptions. First, each single nanofracture test is independent of the previous one; second, each nanoplane forming at a given and known fluence corresponds to a known stress-loading level. The second point has been validated in Ref. [6]. Let us now establish the validity of the first one by studying the statistical nature of the cyclic intermittency between regular and erratic regions of the observed patterns.

To this aim, a number of lines are written at the surface of three brittle materials using a femtosecond laser with varying deposited and pulse energies following a similar approach reported in Ref. [3]. Then, we measure their respective lengths of sections displaying chaotic and regular patterns. The results are shown in Fig. 2, where black domains represent regular regimes (R) and red erratic ones (E), respectively. For fused silica, α-quartz, and sapphire, we systematically observe that as the deposited energy increases both the length and frequency of erratic patterns increase.

In general, intermittent alternations between regular and erratic patterns may arise either in deterministic nonlinear

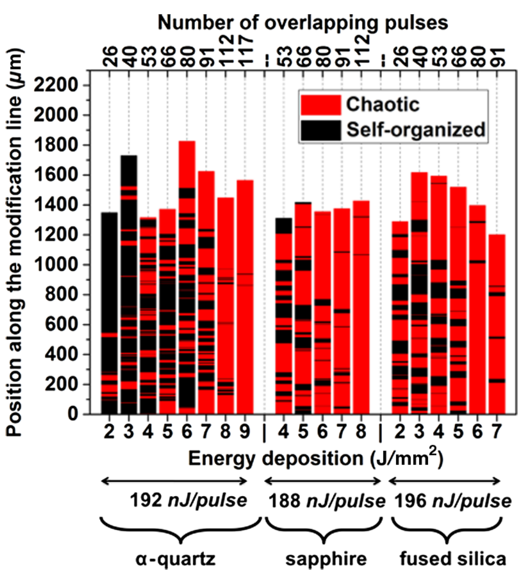

FIG. 2. Overview of the transitions for different energy depositions and pulse energies for three different materials, illustrating the potential universality of this intermittent phenomenon for brittle materials. Black regions represent the self-organized patterns and the red ones the chaotic patterns.

dynamical systems performing transitions from periodic to chaotic evolutions (like in the Pomeau-Manneville scenario [7]) or in stochastic storage systems, where an intrinsic randomness of the incoming and outgoing flows lead to an alternation between "busy" and "idle" periods in the queuing theory [8]. In what follows, we exploit the striking analogy existing between the observed intermittent patterns and the dynamics exhibited by a virtual queuing system (QS). To unveil this analogy, we adopt the Glansdorff-Prigogine generic view [9], and, hence, we consider the laser-glass ensemble to form an open system in which energy is steadily dissipated via several distinct physical mechanisms, one of them being responsible for the generation of the intermittent patterns via an energy-transport mechanism. At this stage, one should realize that such an intermittency arises generically when one studies the dynamics of the waiting-room content of queuing systems. This content randomly alternates between empty and nonempty periods, thus exhibiting a striking analogy with the E and R regimes observed in our patterns. In both cases, a succession of cycles, with a random length duration $C = E + R$, is spontaneously generated by the underlying dynamics. One may now raise the question: Are the random lengths of these successive cycles (C) statistically independent?

Adopting the QS metaphor, one basically assumes that part of the laser-energy pulses are stored into the glass and then released via a pattern-generation mechanism, in the same way a waiting room "storing" incoming customers is purged by delivering a service. Therefore, we emphasize that, in the physical system, the QS virtual customers should not be interpreted as single laser pulses *but as a sequence of them*, leading, for instance, to the formation of nanogratings lamella. From the general QS theory, we know that the server dynamic state alternates between two states, the so-called idle periods (IPs) arising when the waiting room is empty and the busy periods (BPs). In the physical system, idle periods and busy periods correspond microscopically to periodic patterns, formed of nanoplanes, and to erratic patterns, consisting of random cracks, respectively.

Let us call I the time interval duration of an IP, while Θ stands for a BP. Both I and Θ are random variables which, as we shall establish now, are statistically independent; this will be experimentally verified *a posteriori*.

From microscopic observations, we note that the spacing between nanoplanes appearing in the regular portion of the patterns is essentially independent of the pulse energy delivered by the laser [3]. Considering this spacing, we may now define a natural characteristic length scale and its related time scale $t_0 := w_L/v_0$, where v_0 is the translation velocity of the laser. Let us also introduce $\lambda \in [0, 1]$ to be the probability that a BP starts (or, equivalently, an IP ends) in the next time slot t_0. Accordingly, $\text{prob}\{I = k\} = \lambda^{(k-1)}(1 - \lambda)$ stands for the geometric probability law to

TABLE 1. Summary of the Geo/G/1 queuing theory results for α-quartz, sapphire, and fused silica. For the calculations, measured values of $E\{\Theta_i\}$ and ρ_i are used to validate the left and the right parts of Eq. (4). When these values coincide, the system follows the dynamics of the Geo/G/1 QS. Values within an absolute difference of 0.15 are represented in green colour while outliers are represented in red colour.

α-Quartz			*Sapphire*			*Fused silica*		
192 nJ			***188 nJ***			***196 nJ***		
0.94	0.89	0.05	0.68	0.68	0.00	0.59	0.65	0.06
0.70	0.73	0.03	0.85	0.99	0.14	0.77	0.69	0.08
0.77	0.66	0.11	0.62	0.84	0.22	0.24	0.25	0.01
0.24	0.15	0.09	0.68	0.60	0.08	0.50	0.60	0.10
$E\{\Theta_i\}/E\{\Theta_j\}$	**$(1/\rho_i)/(1/\rho_j)$**	**Absolute difference**	0.55	0.21	0.34	**$E\{\Theta_i\}/E\{\Theta_j\}$**	**$(1/\rho_i)/(1/\rho_j)$**	**Absolute difference**
			0.22	0.14	0.08			
			$E\{\Theta_i\}/E\{\Theta_j\}$	**$(1/\rho_i)/(1/\rho_j)$**	**Absolute difference**			

observe an IP of duration k. For this geometric probability law, the average IP duration is $E\{I\} = \lambda^{-1}$ and its variance reads $\sigma_a^2 = (1-\lambda)/\lambda^2$. Our abstract QS metaphor dictates to identify the beginning of the BP with the arrival of a virtual customer in a QS Geo/G/1 queue (see Appendix B for a short review of QS). From Ref. [8], the first two moments of the busy period Θ of the Geo/G/1 queue are explicitly known and read

$$E\{\Theta\} = \frac{1}{\mu(1-\rho)},$$
$$\sigma_\Theta^2 = E\{\Theta^2\} - [E\{\Theta\}]^2 = \frac{\sigma_s^2}{(1-\rho)^3}, \qquad (2)$$

where $\rho = \lambda/\mu \in [0, 1]$ is the QS offered traffic. The parameter $1/\mu$ is associated with the energy-dissipation rate and practically can be realized as an abstract average service-time length. Note that, for the abstract QS, all times appearing in Eq. (2) are now expressed in the natural time units t_0. As for an alternative stochastic process in general and hence for the Geo/G/1, the $E\{I\} = \lambda^{-1}$, we have [10]

$$\rho = \frac{E\{\Theta\}}{E\{I\} + E\{\Theta\}}. \qquad (3)$$

Equation (3) implies that ρ can be measured directly from the experimental patterns in Fig. 2. In addition, keeping μ fixed but varying the traffic λ (i.e., the delivered deposited energy), the first line of Eq. (2) implies

$$\frac{E\{\Theta_1\}}{E\{\Theta_2\}} = \frac{1-\rho_2}{1-\rho_1}, \qquad (4)$$

where Θ_k and ρ_k for $k = 1, 2$ stand for two different BPs resulting from two different traffic loads.

Accordingly, whenever (up to experimental errors) the equality Eq. (4) is satisfied for a set of experiments, one can conclude that the hypotheses underlying our abstract Geo/G/1 picture holds. If this is the case, further conclusions can be drawn:

(a) A single μ exists and it characterizes the typical energy dissipation rate that can be associated to the R/E pattern generation.

(b) Most importantly, the basic hypothesis underlying the QS theory is realized. Since these conditions are fulfilled, the successive busy (BPs) and idle periods (IPs) as well as their alternation are statistically independent.

The experimental validity for three different materials is expressed by Eq. (4) and is summarized in Table 1. This validates our abstract QS metaphor explicitly, and it is reasonable to assume that each nanoplane forms a statistically independent fracture test experiment.

III. MICROSCOPIC MODELING

Let us now examine the microscopic aspect of the intermittency, and more specifically the mechanism of crack formation, which clearly triggers the transition to an erratic regime. Interestingly, the laser-deposited energy and the stress in the material are related as shown in Fig. 3(b).

In previous work, we have demonstrated that the formation of nanogratings is accompanied by a net volume expansion [6], which generates a significant amount of stress in the material. We also know that an increasing deposited energy on the material corresponds to the linear increase of the stress [5] as shown in Fig. 3. The material becomes porous [11] and expands [6],

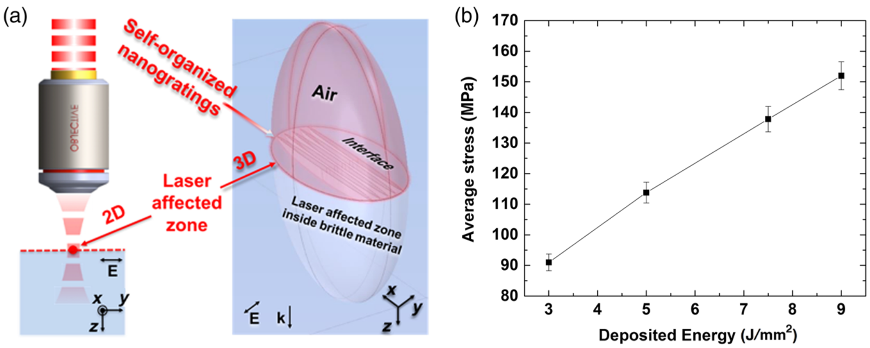

FIG. 3. (a) Schematic illustration of the femtosecond laser ellipsoid which corresponds to the laser-affected volume. The waist of the ellipsoidal is focused on the material-air interface, producing patterns on the surface of the material. (b) The average stress between the nanoplanes in fused silica for the case of 196 nJ per pulse at 800 kHz. The deposited energy is "tuned" by changing the translation velocity of the laser.

generating compressive stress around the laser-affected zones. A high stress concentration is found at the tip of these nanoplanes, where the stress gradient is the highest. This hypothesis is also supported by atomic-force-microscope measurements [12] indicating the interface of the laser-affected and unaffected zones as prone to crack nucleation and formation.

The formation of individual elements of a pattern (nanoplane) is a tensile test at the nanoscale. The maximum stress is found at the tip of the nanoplane and, in a first approximation, is given by the Inglis formula [13]: $\sigma_{\max} = \sigma_{\text{avg}}(1 + 2a/b)$. Parameters σ_{avg}, a, and b are the average stress between the lamellae and geometrical factors, respectively [see Fig. 4(b)]. Based on previous work [6], the average stress within nanoplanes as a function of the deposited energy can be precisely determined for each specific laser exposure condition and is found to linearly increase with the amount of energy deposited in the material [Fig. 3(b)]. Note that the material tested is the material close to, but yet outside, the laser-exposed zone.

Each single experiment *per se* can have two outcomes: either one regular nanoplane formation or the nucleation of a crack, respectively. If we assume a strict independence between loading events as discussed in the previous paragraphs, the number of experiments taking place before failure occurs can be formulated mathematically by the geometric distribution $\text{prob}\{r = n\} = p(1 - p)^{n-1}$, where r is the number of experiments performed in one experimental cycle (defined as C in our QS model) and p is the probability of a failure to happen.

In the brittle materials considered here, one cannot precisely define the elastic limit above which the material ruptures. The probability of failure under a given stress is commonly described by a Weibull statistical law [4]. Combining the Weibull law with the average of geometric distribution, we get the following equation:

$$\underbrace{\ln\left[-\ln\left(1 - \frac{1}{\bar{r}}\right)\right]}_{y} = \underbrace{m\ln\sigma}_{mx} - \underbrace{\left[m\ln\sigma_N + \ln\left(\frac{V}{V_0}\right)\right]}_{\beta}. \tag{5}$$

The equation is defined by two parameters: the scale parameter, which has the same dimensions as a stress, and the dimensionless factor m (also called the Weibull modulus). For the case of fused silica, the average number of nanoplanes ($\langle\bar{r}\rangle$) is measured using SEM images like the ones shown in Fig. 2. Parameters V and V_0 are needed in order to take into account the different sizes of these stretched ellipsoidal nanoplanes as the energy per pulse increases.

By linearly fitting the data points, a visual assessment of the validity of the initial hypothesis—"nanoplanes form independent tensile tests"—is provided. As shown in Fig. 5, the experimental data form a single straight line in accordance with Eq. (5) with convincingly high levels of confidence. The maximum stress for our mechanical tests reaches 1.7 GPa. This value is consistent with previously reported ones both in silica fibers produced by fusion splicing [14] as well as for fused silica mechanical parts processed via femtosecond laser exposure and chemical etching [15,16].

The theoretical strength value of bulk fused silica to fail is estimated in the order of 21 GPa, indicating that it fails due to the presence of flaws on its surface. It has been reported that chemical etching in hydrofluoric acid of silica

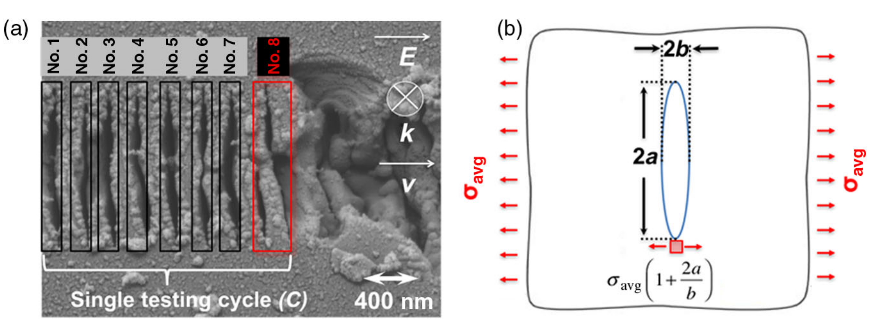

FIG. 4. (a) Each element formation can be seen as an individual tensile-stress loading experiment. A testing cycle (C) is terminated a fracture occurs. (b) Illustration of the loading conditions for a single nanoplane formalized as an Inglis fracture problem [13].

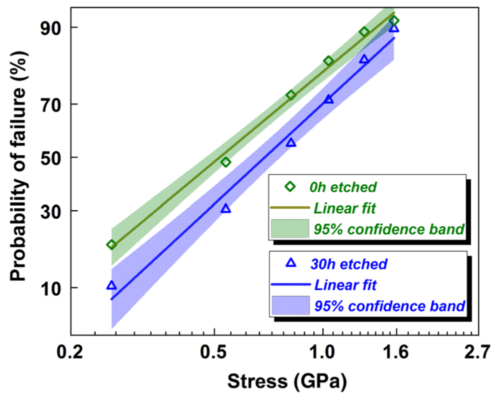

FIG. 5. The graph represents the probability of fused silica to fail under a certain stress level. The two curves correspond to two different surface qualities. For both cases, the 95% confidence band is given by the equation $x \pm Z \times \sigma/\sqrt{(n)}$, where Z is the confidence level, σ is the standard deviation, and n is the sample size. For the two cases, the relative error along the x axis is 3% of the values and finds its origin in the evaluation of the average stress between the nanoplanes (see Fig. 4). The relative error along the y axis is estimated to be 5% of the values and is related to the uncertainty of the start position of the transition towards an erratic regime. For the sake of clarity, the error bars are not presented in the graphs.

does improve the mechanical resistance of glass surface [16–18]. This result supports the validity of our hypothesis that every single nanoplane formation is essentially a fracture problem and essentially that the surface quality of the material is mechanically tested.

IV. CONCLUSIONS AND PERSPECTIVES

In summary, we investigate the intermittent behavior when exposing the surface of brittle materials with femtosecond laser pulses. In particular, using the queuing theory, we unravel striking similarities that we use to demonstrate that the formation of each nanoplane is independent of each other. This key finding, in conjunction with our previous knowledge on the stress generation associated with the formation of these nanoplanes, leads us to conjecture that each single lamella formation is equivalent to a single "loading" experiment. Here, we prove that the intermittent behavior finds its roots in the fracture mechanics of the material. From the number of nanoplanes formed before fracturing the material, one can extract important parameters of the glass' surface mechanics such as the Weibull parameters, commonly used for defining the probably of rupture for brittle materials.

In this work, the levels of deposited energy are achieved by an *ad hoc* selection of writing speeds and repetition rates. However, considering the crack propagation dynamics, different patterns of alternating sequences of erratic and organized nanoplanes can be achieved for different pairs of scanning speed or repetition rates, although they yield an identical amount of deposited energy into the material. The origin can be found in the various time scales of the physical phenomena sustaining the formation of these patterns, like, for instance, the plasma dynamics relaxation, the excitons dynamics, the crack nucleation rate, and later propagation in conjunction with the feed rate of pulses as well as the scanning velocity. Furthermore, secondary effects should be investigated, i.e., the shockwave propagation, residual loads, etc.

Overall, this methodology offers a straightforward and contactless method for extracting fracture mechanics data of surfaces at all sizes and with a minimum amount of materials. It opens opportunities for the rapid diagnosis of surface strength, for instance, for quality control of consumer electronics and other fields, a quality control test that is currently hard to implement, but also for further analyzing the behavior of brittle materials at small scales.

ACKNOWLEDGMENTS

The authors acknowledge the financial support of the European Research Council (Galatea project, ERC-2012-StG-307442).

APPENDIX A: EXPERIMENTAL SETUP

Using an Amplitude Systèmes' femtosecond laser with a pulse length of approximately 270 fs and a wavelength of 1030 nm, lines are written to intersect the surface of the different materials. The repetition rate of the laser is 800 kHz, and the velocity of writing is varied to achieve the desired energy deposition, or dosage, using high-precision linear translation stages (PI Micos GmbH). The conditions of exposure are set by fixing the range of energy depositions (dosage) between 2 and 10 $\mathrm{J/mm^2}$ that had previously been identified as likely to produce the most interesting results for the nanogratings. The laser is focused onto the specimen using a 40× objective lens (OFR/Thorlabs) that has an NA of 0.4 creating a maximum modification width of approximately 1.5 μm as observed by the SEM imaging. By slightly varying the depth of the laser track with respect to the surface (with steps of 1 μm) of the specimen, the modification is ensured to cross the surface plane. This method also allows the observation of the material modification at different locations within the focal volume. For the analysis, the tracks which are roughly 50% within the volume of the material are used.

Following the laser writing, a specimen is observed with a scanning electron microscope after a thin coating ($\leq$20 nm) of gold is sputter-coated to create a conductive surface and avoid surface charging that can be induced by the electron microscope.

Statistical analysis of the laser tracks excludes 500 μm from either end to avoid possible changes due to the specimen's edge or stage deceleration (as the end of the track is not continued beyond the specimen's far edge). Moreover, the very low (less than 5%) and very high traffic values (more than 90%) are not included in the data analysis.

APPENDIX B: GEO/G/1 QUEUING SYSTEM

A single QS is a dynamical in which a random flow of incoming customers [i.e., the time interval between two successive incomers is a random variable (RV)] are served, one by one, by a single server. The service duration itself is also a RV. Before being served, the customers are stored in a waiting room in which actual content is a stochastic process. The QS system dynamics can be described in either a discrete or continuous time framework. Basically, a single-server QS, denoted by $A/B/1$, is fully characterized by two probability laws A and B, respectively, describing the statistics of the interarrival and service-time durations. In our case, we make use of a discrete-time, single-server QS written (standardly written as Geo$/G/1$, where the 1 indicates that a single server works) for which the arrivals are drawn from a geometric probability law *geo* with parameter λ and the service duration is a general RV G with μ^{-1} and σ_s^2 for the average and the variance, respectively.

[1] Y. Shimotsuma, P. G. Kazansky, J. Qiu, and K. Hirao, Self-Organized Nanogratings in Glass Irradiated by Ultrashort Light Pulses, Phys. Rev. Lett. **91**, 247405 (2003).
[2] V. R. Bhardwaj, E. Simova, P. P. Rajeev, C. Hnatovsky, R. S. Taylor, D. M. Rayner, and P. B. Corkum, Optically Produced Arrays of Planar Nanostructures inside Fused Silica, Phys. Rev. Lett. **96**, 057404 (2006).
[3] N. Groothoff, M. O. Hongler, P. G. Kazansky, and Y. Bellouard, Transition and self-healing process between chaotic and self-organized patterns observed during femtosecond laser writing, Opt. Express **23**, 16993 (2015).
[4] W. Weibull, Statistical distribution function of wide applicability, J. Appl. Mech. **18**, 293 (1951).
[5] A. Champion, M. Beresna, P. G. Kazansky, and Yves Bellouard, Stress distribution around femtosecond laser affected zones: Effect of nanogratings orientation, Opt. Mater. Express **21**, 24942 (2013).
[6] A. Champion and Y. Bellouard, Direct volume variation measurements in fused silica specimens exposed to femtosecond laser, Opt. Express **2**, 789 (2012).
[7] Y. Pomeau and P. Manneville, Intermittent transition to turbulance in dissipative dynamical systems, Commun. Math. Phys. **74**, 189 (1980).
[8] H. Takagi, *Queueing Analysis: Discrete-time systems*, 1st ed. (North-Holland, Amsterdam, 1991).
[9] P. Glansdorff and I. Prigogine, *Thermodynamic Theory of Structure, Stability and Fluctuations* (Wiley-Interscience, New York, 1971).
[10] J. Medhi, *Stochastic Models in Queuing Theory*, 2nd ed. (Academic, New York, 2002).
[11] J. Canning, M. Lancry, K. Cook, A. Weickman, F. Brisset, and B. Poumellec, Anatomy of a femtosecond laser processed silica waveguide, Opt. Mater. Express **1**, 998 (2011).
[12] Y. Bellouard, E. Barthel, A. A. Said, M. Dugan, and P. Bado, Scanning thermal microscopy and Raman analysis of bulk fused silica exposed to low-energy femtosecond laser pulses, Opt. Express **16**, 19520 (2008).
[13] C. E. Inglis, Stresses in a plate due to the presence of cracks and sharp corners, Trans. Inst. Nav. Arch. **55**, 219 (1913).
[14] C. R. Kurkjian, J. T. Krause, and M. J. Matthewson, Strength and fatigue of silica optical fibers, J. Lightwave Technol. **7**, 1360 (1989).
[15] C. E. Athanasiou and Y. Bellouard, A monolithic microtensile tester for investigating silicon dioxide polymorph micromechanics, fabricated and operated using a femtosecond laser, Micromachines **6**, 1365 (2015).
[16] Y. Bellouard, On the bending strength of fused silica flexures fabricated by ultrafast, Opt. Mater. Express **1**, 816 (2011).
[17] N. H. Ray and M. H. Stacey, Increasing the strength of glass by etching and ion-exchange, J. Mater. Sci. **4**, 73 (1969).
[18] L. G. Baikova and V. P. Pukh, The effect of the type of chemical treatment on the strength of silica and silicate glasses, Glass Ceram. **30**, 834 (1973).